Advances in Military Technology
Vol. 21, No. 1, 2026, pp. 195-212
ISSN 1802-2308, eISSN 2533-4123
DOI 10.3849/aimt.02053

Influence of Certain Structural Parameters on the Firing Stability of the Robot-Weapon System on Elastic Ground

D. Ba Ngoc[1*], M. Macko[1], B. Viet Dung[1], and V. Van Bien[2]

[1] *Department of Weapon and Ammunition, University of Defence, Brno, Czech Republic*
[2] *Department of Weapons, Le Quy Don Technical University, Hanoi, Vietnam*

The manuscript was received on 5 November 2025 and was accepted after revision for publication as an original research paper on 4 April 2026.

Abstract:

In this paper, a small-caliber automatic weapon mounted on a combat robot is chosen as the research subject to analyze firing stability. A dynamic model with six degrees of freedom is formulated based on Lagrange's equation of the second kind and multi-body system theory, accounting for the elastic response of the ground. Recoil forces induced by firing, which excite the whole system, are determined experimentally for single shots and three-round short bursts. The study also examines the influence of certain representative structural parameters on the firing-induced vibrations of the complete mechanism. The obtained results provide a basis for assessing firing accuracy and contribute to the design, manufacture, and operational employment of this weapon system on the battlefield.

Keywords:

robot system, unmanned ground vehicle (UGV), firing stability, structural parameters

1 Introduction

Nowadays, with the rapid development of science and technology, significant advancements have been made in the military sector. One notable achievement is the successful fabrication of combat vehicles that can operate without direct human intervention, thereby reducing casualties on the battlefield. These vehicles are commonly known as military robots. In modern warfare, military robots, particularly unmanned ground vehicles (UGVs), are gaining increasing attention. UGVs are ground-based robots that can operate without a human operator inside. They can be remotely controlled or operate autonomously using artificial intelligence (AI), sensors and positioning systems developed by militaries worldwide, including Vietnam. Research-

* *Corresponding author: Deparment of Weapon and Ammunition, University of Defence, Kounicova 156/65, CZ-662 10 Brno, Czech Republic. Phone: +420 608 505 456, E-mail: bangoc.dang@unob.cz. ORCID 0009-0006-0481-4572.*

ers at Weapons Institute have conducted studies in this field and have successfully developed armed military robots capable of performing critical missions. This platform features six wheels and consists of two main parts: the robot body, which includes the chassis, aiming mechanism, orientation mechanism, wheels; and the weapon system, which is a small-caliber automatic firearm, specifically the compact submachine gun, see Fig. 1. However, the product is still in the testing phase and the robot's parameters, such as mobility speed, weapon firing rate, firing stability and shooting accuracy, are still being refined.

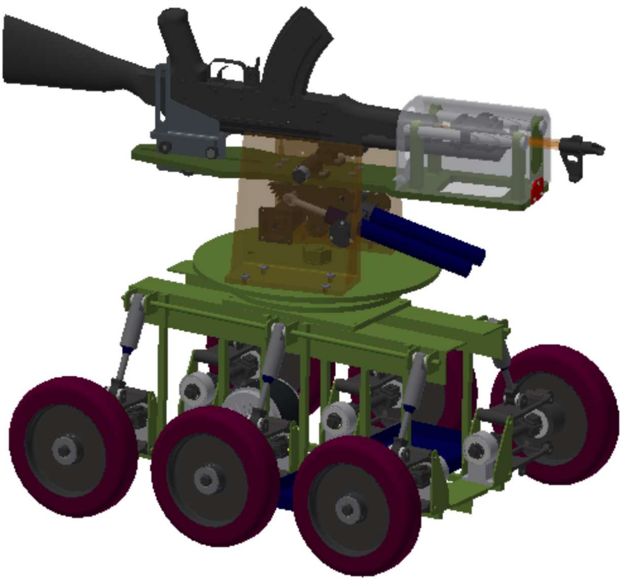

Fig. 1 Military robot bears automatic weapon

The study of the dynamics of automatic weapons mounted on robots during firing is a pressing task that requires focused attention. The results will provide a scientific basis for further research, improvement, design, and manufacture of such weapon systems. Several studies have been published on the dynamics of weapons mounted on ground combat vehicles. The most notable among these are presented in [1–6]. However, previous studies have overlooked the operation of the automatic mechanism simultaneously with the motion of the entire system, and the evaluation of the influence of certain structural parameters of the robot on system stability during firing has not been addressed.

Balla et al. [1, 2] established dynamic models of weapon systems installed on tracked vehicles, while according to the study [3], Huai-Ku Sun et al. utilized the finite element method to examine the vibrations of a machine weapon mounted on a four-wheeled vehicle. However, these studies only considered vibration components in the vertical plane and were unable to fully describe the spatial dynamics of the mechanism. The suspension systems were simplified and the model only accounted for three degrees of freedom (vertical displacement Z, and rotational displacements θX, θY), neglecting longitudinal and lateral forces from the wheels, see in [4]. Additionally, the automatic firing system's operation was not taken into consideration, the dynamics of the automatic weapon mounted on the vehicle are not considered simultaneously with the system vibrations induced by the firing forces. This is a crucial aspect of automatic weapons and has a significant impact on the firing stability of the system. To address these limitations, this paper presents a dynamic model of an automatic gun mounted on an UGV, specifically for an automatic gun operating on the gas-operated principle. The model is developed using Lagrange's equations of motion and takes into account the simultaneous operation of the automatic mechanism with the system's motion. Currently, there is a lack of complete and reliable theoretical foundation to support the exploitation, improvement, and design of UGVs. Therefore, this paper aims to provide a detailed study on the firing stability of UGVs.

Furthermore, the paper establishes a generalized model of the spatial vibrations of the robot-weapon system during firing. This model provides a theoretical basis for determining key structural parameters of combat robots equipped with small-caliber automatic weapons in order to ensure firing stability. It also serves as a scientific foundation for the calculation and optimization of the design of modern small-caliber infantry weapons when integrated into intelligent robotic platforms, thereby enabling the development of new weapon systems with enhanced firepower and improved combat effectiveness on the battlefield.

2 Dynamic Model

The UGV model with 6 degrees of freedom investigated in this study is based on the Lagrangian differential equations and uses an integrated model of several subsystems to describe the motion of the mechanical system, including the ride model and the firing force model.

2.1 Ride Model

The wheeled vehicle robot model is designed with three wheels on the right side and three wheels on the left side, see in Figs 2 and 3. The automatic weapon is mounted on the vehicle through range, directional joints and the shock absorber system. A wheeled vehicles robot model has been established in this study by using the following assumptions:

- details and detail assemblies are considered absolute solids, the symmetry axes pass through the center of each object. Ignoring gaps and friction in the joints, the linkages are locked firmly during firing,
- the wheeled vehicle robot is assumed to be stationary during firing. The elevation angle and traverser angle are constant,
- the wheels are replaced by springs with stiffness k_t and dampers with viscous damping coefficient c_t; suspension system is replaced by spring with stiffness k_s and damping with viscous resistance coefficient c_s and just vertically,
- the ground is flat and represented as a linear spring with stiffness k_g, the drag and friction forces are evenly applied to the wheels.

Based on the physical architecture of the system, the interconnections among the combat robot's subsystems, and the stated modeling assumptions, a multi-body dynamic model of the combat robot was formulated (Figs 2 and 3). The combat vehicle is assumed to be positioned on a flat surface, and in the initial state, no external force components – including gravitational effects – are applied to the system.

DOI 10.3849/aimt.02053

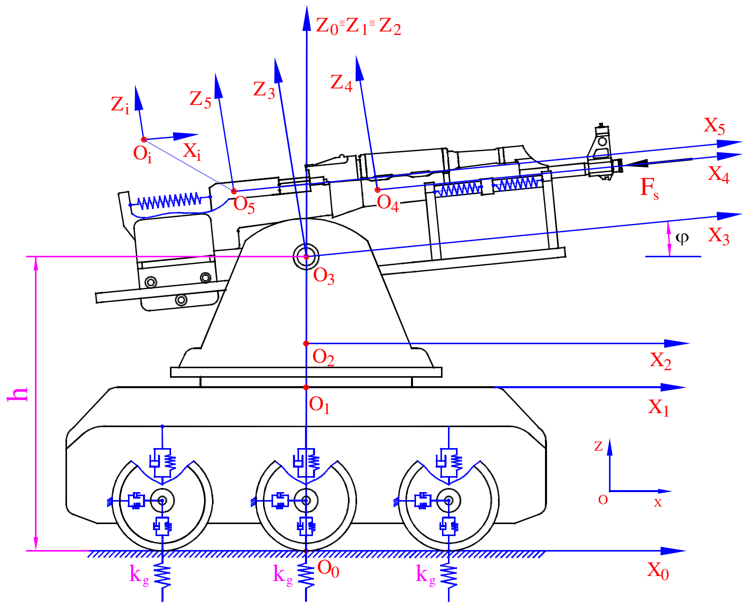

Fig. 2 Dynamic model of robot UGV – side view

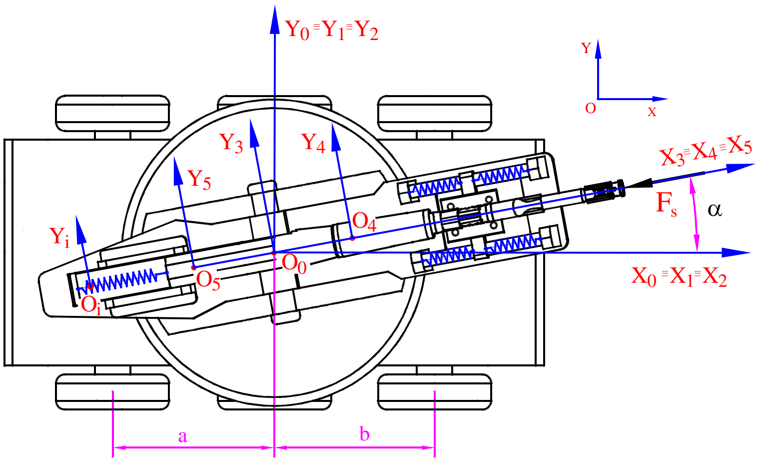

Fig. 3 Dynamic model of robot UGV – overhead view

The combat vehicle robot system consists of 5 rigid bodies: vehicle body (body 1); traverser parts (body 2); elevation parts (body 3); weapon frame (body 4); breech system (body 5). In addition, there are working mechanisms of the automatic machine whose motion depends on the movement of the base link, which is the breech (body *i* with *i* =1, 2, 3…). To investigate the system of rigid body dynamics, bodies of the system were attached in a Cartesian coordinate system as shown in Figs 2 and 3, where

- $O_0X_0Y_0Z_0$ represents the stationary coordinate system fixed on the ground,

- $O_kX_kY_kZ_k$: accounts for the local coordinate system established at the k-th rigid body, for $k = 1,..., 5$.

From the assumptions and layout of objects, the combat vehicle robot system has 6 independently generalized coordinates, where

- q_1 – the translational displacement body 1 along O_0X_0 – axis; q_2 – the translational displacement body 1 about O_0Z_0 – the axis; q_3 – the bounce angle body 1 about O_0X_0 – the axis; q_4 – the bounce angle body 1 about O_0Y_0 – the axis; q_5 – the translational displacement body 4 along O_3X_3 – the axis; q_6 – the translational displacement of body 5 along O_4X_4 – the axis,
- q_i – the translational displacement of body i along O_iX_i [m] – the axis are dependent generalized coordinates.

Since Body 5 serves as the base link that transmits motion to the working links, each connected link is modeled with an equivalent reduced mass m_i^* [kg], transmission ratio K_i, and an efficiency η_i. As body 5 moves along their travel paths, it sequentially engage and disengage with the working links. Therefore, the reduced mass of body 5 also changes during the operation.

$$m_5 = \left(m_{\text{recoiling mass}} + \sum_{i=1}^{n} \frac{K_i^2}{\eta_i} m_i^* \right) \frac{\mathrm{d}q_6}{\mathrm{d}t} \tag{1}$$

Kinetic Energy of the Robot System

In the theory of multibody mechanical systems [7], the translational Jacobian matrix and the rotational Jacobian matrix are introduced, as expressed in equations (2) and (3), specifically:

$$J_{Ti} = \frac{\partial r_i}{\partial q} = \begin{bmatrix} \frac{\partial r_{ix}}{\partial q_1} & \frac{\partial r_{ix}}{\partial q_2} & \cdots & \frac{\partial r_{ix}}{\partial q_6} \\ \frac{\partial r_{iy}}{\partial q_1} & \frac{\partial r_{iy}}{\partial q_2} & \cdots & \frac{\partial r_{iy}}{\partial q_6} \\ \frac{\partial r_{iz}}{\partial q_1} & \frac{\partial r_{iz}}{\partial q_2} & \cdots & \frac{\partial r_{iz}}{\partial q_6} \end{bmatrix} \tag{2}$$

$$J_{Ri} = \frac{\partial \omega_i}{\partial \dot{q}} = \begin{bmatrix} \frac{\partial \omega_{ix}}{\partial \dot{q}_1} & \frac{\partial \omega_{ix}}{\partial \dot{q}_2} & \cdots & \frac{\partial \omega_{ix}}{\partial \dot{q}_6} \\ \frac{\partial \omega_{iy}}{\partial \dot{q}_1} & \frac{\partial \omega_{iy}}{\partial \dot{q}_2} & \cdots & \frac{\partial \omega_{iy}}{\partial \dot{q}_6} \\ \frac{\partial \omega_{iz}}{\partial \dot{q}_1} & \frac{\partial \omega_{iz}}{\partial \dot{q}_2} & \cdots & \frac{\partial \omega_{iz}}{\partial \dot{q}_6} \end{bmatrix} \tag{3}$$

where J_{Ti} is the translational Jacobian matrix; J_{Ri} is the rotational Jacobian matrix.

The generalized mass M_q matrix of the system is [7]:

$$M_q = m_i J_{Ti}^{\mathrm{T}} J_{Ti} + J_{Ri}^{\mathrm{T}} I_{i0} J_{Ri} \tag{4}$$

where m_i is the mass of the i-th rigid body i [kg]; $I_{i0} = A_i I_i A_i^{\mathrm{T}}$ is the inertia tensor with respect to the center of mass of each body in the inertial frame O_0; A_i is the direction cosine matrix of the i-th rigid body; A_i^{T} is the transpose of the matrix A_i; I_i is the inertia tensor in the body-fixed coordinate system attached to body i.

Therefore, the kinetic energy T of the multibody system is given by [7]:

$$T = \frac{1}{2}\frac{\mathrm{d}q^{\mathrm{T}}}{\mathrm{d}t} M_q \frac{\mathrm{d}q}{\mathrm{d}t} \tag{5}$$

Forces Acting on the Weapon Robot System

In studies [8–10], virtual work of generalized force F_k and torque M_k are calculated as follows:

$$\delta W_1 = \sum_{j=1}^{6}\left[\sum_{k=1}^{5} F_k^T \frac{\partial R_k}{\partial q_j}\right]\delta q_j \tag{6}$$

$$\delta W_2 = \sum_{j=1}^{6}\left[\sum_{k=1}^{5} M_k^T \frac{\partial \theta_k}{\partial q_j}\right]\delta q_j \tag{7}$$

where δW_1 is the virtual work produced by the force F_k; δW_2 is the virtual work produced by the moment M_k.

When the link is modeled as an ideal constraint and friction is neglected, the constraint force (i.e., the reaction force associated with the constraint) performs no virtual work; hence, its potential work is zero.

$$P_j = \sum_{k=1}^{5} F_k^{\mathrm{T}} \frac{\partial R_k}{\partial q_j} \tag{8}$$

$$P_j = \sum_{k=1}^{5} M_k^{\mathrm{T}} \frac{\partial \theta_k}{\partial q_j} \tag{9}$$

where P_j – the generalized force corresponding to the generalized coordinates q_j [N]; generalized force F_k impacts the object k-th respectively, include

- the gravity of the bodies (P_k)

Gravity applied to the k-th object has a point set at the center of the object, perpendicular to the horizontal OXY plane and direction to the bottom.

$$P_k = m_k g \tag{10}$$

where m_k the mass of the k-th body [kg]; g is the gravitational acceleration ($g = 9.81$ m/s^2),

- the visco-elastic force of the suspension system (F_{v})

F_{vfr}, F_{vfl}, F_{vmr}, F_{vml}, F_{vrr}, and F_{vrl} are the visco-elastic force of the suspension system at front right and front left, middle right and middle left, rear right and rear left, respectively, they are calculated [11]:

$$F_{\mathrm{v}} = k_{\mathrm{v}}\left(x_{0\mathrm{v}} + \delta x_{\mathrm{v}}\right) + c_{\mathrm{v}}\,\delta \dot{x}_{\mathrm{v}} \tag{11}$$

where k_{v} is the stiffness of suspension springs [N/m]; $x_{0\mathrm{v}}$ is the initial compression of suspension springs [m]; c_{v} is the resistance coefficient of suspension [N·s/m]; δx_{v} is the deviation of the elastic element vector of the suspension spring [m],

- the force of the wheels (F_w)

F_{wfr}, F_{wfl}, F_{wmr}, F_{wml}, F_{wrr} and F_{wrl} are the tire forces at front right, front left, middle right, middle left, rear right and rear left, respectively. They are determined by the following formula:

$$F_w = k_{ss}\left(x_{0w} + \delta x_w\right) + c_w \delta \dot{x}_w \tag{12}$$

where x_{0w} is the initial compression of tires springs [m]; δx_w is the deviation of the elastic element vector of the tire-replacement spring [m]; c_w is the resistance coefficient of tire [Ns/m]; k_{ss} denotes the equivalent stiffness coefficient of the series connection between the elastic component representing the rubber tire and the elastic components modeling the ground [N/m]. According [12] its value was determined using the following relationship.

$$k_{ss} = \frac{k_t\, k_g}{\left(k_t^{\frac{2}{3}} + k_g^{\frac{2}{3}}\right)^{\frac{3}{2}}} \tag{13}$$

where k_t – the rubber band stiffness [N/m]; k_g – the ground stiffness [N/m].

The ground stiffness was caculated by the following dependency:

$$k_g = \frac{E_0}{\omega B\left(1-\varepsilon^2\right)}$$

Whereas the rubber band stiffness with the following expression:

$$k_t = \frac{\sqrt{32}\, E b \sqrt{r_1}}{3h}$$

where E_0 – Young's modulus of the firing ground soil [Pa], ω – the caterpillar tread shape factor, B – the caterpillar tread width [m], ε – the ground side expansion factor, E – Young's modulus for rubber [Pa], h – the rubber band height [m], b – the rubber band width [m], r_1 – the wheel radius along with band [m].

According to study [13], Young's modulus of the firing ground soil E_0 is determined by the following formula:

For cohesive soil:

$$E_0 = 1.0213\times10^5\,[2.97-e]^2\,\frac{\sqrt{\frac{\sigma_{zi}}{3}\left(\frac{1+\nu}{1-\nu}\right)}}{1+e}$$

For loose soil:

$$E_0 = 2.184\times10^5\,[2.17-e]^2\,\frac{\sqrt{\frac{\sigma_{zi}}{3}\left(\frac{1+\nu}{1-\nu}\right)}}{1+e}$$

where $\sigma_{zi} = R_{zi}/A_j$ – the compressive stress [N/m^2]; R_{zi} – the force acting at the wheel [N]; A_j – the contact area between the wheel and the ground [m^2]; ν – the Poisson's ratio; e – the dependent coefficient.

- the shock absorber system of the robot system consists of 2 similar mechanisms which are placed symmetrically through the firing plane. Each mechanism consists of two coaxial springs together. These springs act in opposite directions. Force of the shock absorber (F_a) include F_{ar}, F_{al} – the forces of the shock absorber at right and left, respectively.

$$F_a = k_{af}\left(x_{0af} + q_5\right) + k_{ar}\left(-x_{0ar} + q_5\right) \tag{14}$$

where k_{af} – the stiffness of the front spring [N/m]; k_{ar} – the stiffness of the rear spring [N/m]; x_{0af} – the initial compression of the front spring at the equilibrium state [m]; x_{0ar} – the initial compression of the rear spring at the equilibrium state [m].

- the force of shot (F_s) transmitted from an automatic weapon to a mount is determined in section 2.2.

The problem about calculating the vibration of the combat vehicle robot system establishes equations using Lagrange equations of the second kind, see section D of page 2 [9] and see section 3 of page 3 [14]. The matrices formula of equations is written:

$$\frac{\mathrm{d}}{\mathrm{d}t}\left(\frac{\partial T}{\partial \dot{q}_j}\right) - \frac{\partial T}{\partial q_j} = P_j \quad j = 1, \cdots, 6 \tag{15}$$

where T – the total kinetic energy of the whole mechanical system [kg·m^2/s^2].

2.2 Force of Shot F_s Model

In this study, the UGV was equipped with an AKM submachine gun. The forces acting on the gun during firing, along with the method for their determination, are presented in reference [15–17]. The resultant of these force components is transmitted from the gun to the robot and constitutes the primary source of vibrations in the entire system. The schematic layout for determining the recoil force of the gun is illustrated in Fig. 4.

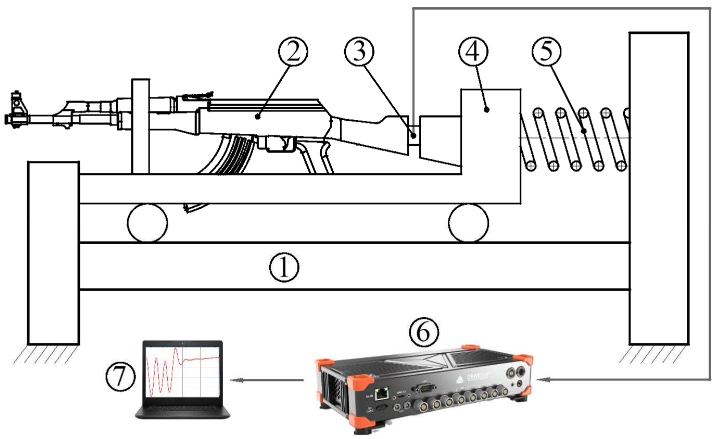

Fig. 4 Diagram of the firing force measurement system. 1. Fixed frame; 2. Gun; 3. LB 15K force sensor; 4. Movable support frame; 5. Recoil damping spring; 6. Data acquisition and processing system; 7. Signal display device

The firearm is mounted on a specialized fixture, and the force sensor is attached to the gunstock, ensuring that the sensor's axis aligns with the barrel axis. The gun is fired using an indirect trigger mechanism, thereby completely eliminating unintended inputs from the shooter. The measured signal is transmitted to the data acquisition and processing system and output to a display device in graphical form. The recoil force measurement test setup consists of the following components:

- the LB 15K force sensor and the SIRIUSiXHS-8xACC data acquisition and signal processing system. The LB 15K force sensor operates on the principle of elastic deformation. The force applied is detected by the sensor and converted into an electrical signal, which is then transmitted to the data acquisition and processing system. The key specifications of the LB 15K force sensor include the measurement range of 0 lbs to 15 000 lbs; the operating frequency range of 0 Hz to 1 000 Hz; the operating temperature of −10 °C to 100 °C; the accuracy-of 0.2 %; sensitivity: 2 mV/V,
- the SIRIUSi-XHS-8xACC data acquisition and signal processing system is an independent 8-channel DAQ designed to measure IEPE/ICP sensors. This DAQ device is ideal for the most demanding real-time data recording applications. It utilizes the new HybridADC technology, enabling two operating modes: high-bandwidth acquisition at a sampling rate of 15 MHz, or high dynamic range acquisition with up to 150 dB dynamic range at a lower sampling rate.

The experimental setup is shown in Fig. 5. After conducting the measurements, the signal from the force sensor is transmitted to the signal acquisition and processing system. The measurement results are presented in Figs 6 and 7.

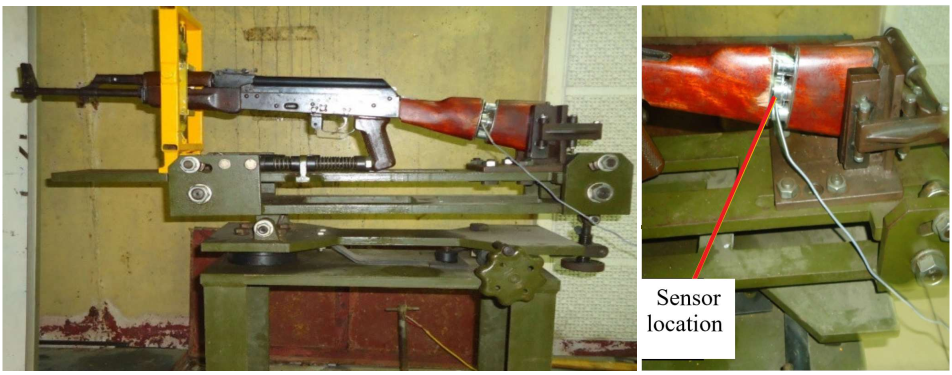

Fig. 5 Experimental measurement of gun recoil force

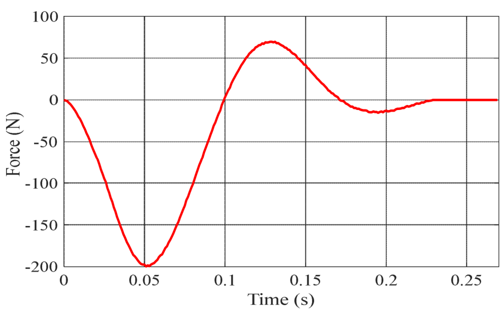

Fig. 6 Measurement of recoil force during-single-shot firing

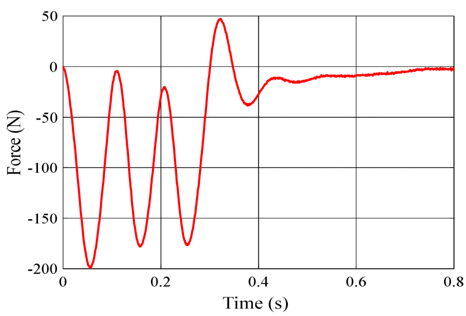

Fig. 7 Measurement of recoil force during three-round burst firing

The results obtained from the experiment has been simulated using the dynamic model of the robot weapon system presented in section 2.1 to evaluate firing stability.

2.3 General Differential Equations System

After determining the kinetic energy (U) and the generalized forces (P_j) of the robot-weapon system, a seven-equation system of second-order differential equations is obtained using the Lagrange formulation Eq. (15). Using dynamic links of elements i with body 5 (Base link) through the transmission ratio K_i and performance η_i, according to [8] we have the following relationship:

$$\dot{q}_i = k_i \dot{q}_6 \quad \text{so, thus} \quad \dot{q}_i = k_i\,\dot{q}_6 + \dot{q}_6 \frac{\mathrm{d}k_i}{\mathrm{d}t}. \tag{16}$$

$$\frac{\mathrm{d}k_i}{\mathrm{d}t} = \frac{\mathrm{d}k_i}{\mathrm{d}q_6}\frac{\mathrm{d}q_6}{\mathrm{d}t} = \dot{q}_6 \frac{\mathrm{d}k_i}{\mathrm{d}q_6} \quad \text{so} \quad \ddot{q}_i = k_i\,\ddot{q}_6 + \dot{q}_6^2 \frac{\mathrm{d}k_i}{\mathrm{d}q_6} \tag{17}$$

On the other hand we have:

$$\eta_i = \frac{R_i^{'}}{R_5^{'}} \cdot \frac{\mathrm{d}q_i}{\mathrm{d}q_6} = \frac{R_i^{'}}{R_5^{'}} \cdot k_i \quad => \quad R_5^{'} = \frac{k_i}{\eta_i} R_i^{'} \tag{18}$$

where $R_5^{'}$, $R_i^{'}$ – the total thrust and drag acting on body 5 and body *i*.

$$R_5^{'} = Q_5 - m_5\,\dot{q}_6 \quad \text{and} \quad R_i^{'} = Q_i + m_i\,\dot{q}_i \tag{19}$$

where Q_5, Q_i are external forces acting on body 5 and body i.

Substituting the expressions from Eqs (16)-(19) into the system of differential equations governing the mechanical system and performing the necessary transformations, we obtain a system of six second-order quadratic differential equations. In this system, the variables are the second time derivatives of the generalized coordinates, which describe the spatial vibrations of the combat robot during firing.

The equation quadratic system (*EQS*) is as follows:

$$EQS = [eq_1, eq_2, eq_3, \ldots, eq_6] \tag{20}$$

3 Simulation Results

To solve the system of Eq. (20), it is first necessary to determine the input parameters of the system, including ballistic parameters required for solving the firing problem as described in [16], structural parameters of the system, and dynamic linkage characteristics of the robot–weapon mechanical system. Dimensional and mass parameters are obtained through direct measurement on the robot or taken from technical specifications. The moments of inertia and center of mass positions are determined using SolidWorks software. The main input parameters of the mechanical system are shown in Tabs 1 and 2.

The system of Eq. (20) is solved in conjunction with the ballistic equations [18], as well as the dynamic equations of the gas-operated automatic firing mechanism described in [19], using Maple software. The dynamic simulation results of the automatic mechanism provide the pressure profiles of the propellant gases in the gas chamber and inside the barrel (Fig. 8), and the motion law of the base link (the breech) of the AKM submachine gun (see Fig. 9).

Tab. 1 Elasticity and damping parameters

Parameters	Symbol	Value
Stiffness coefficient of springs replacing wheels	k_t	(14 500–15 000) N/m
Stiffness coefficient of springs replacing suspension system	k_s	(1 200–1 250) N/m
Stiffness coefficient of recoil reduction springs	k_{af}, k_{ar}	2 000 N/m
Damping coefficient of dampers replacing wheels	c_t	(300–350) N·s/m
Damping coefficient of dampers replacing suspension system	c_s	(250–300) N·s/m
Poisson's ratio of loose soil	v	0.4
Dependent coefficient of loose soil	e	0.52
Density of loose soil	ρ	1 780 kg/m^3

Tab. 2 Mass and moment of inertia of objects in the model

Body	Mass [kg]	J_x [kg·m^2]	J_y [kg·m^2]	J_z [kg·m^2]
Vehicle body	40.00	0.67000	2.8300	3.2300
Traverser parts	1.51	0.01800	0.0180	0.0140
Elevation parts	2.15	0.02300	0.0230	0.0340
The weapon frame	3.24	0.00042	0.0127	0.0093

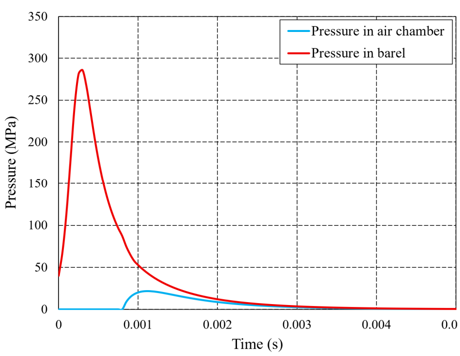

Fig. 8 Pressure in the barel and gas chamber

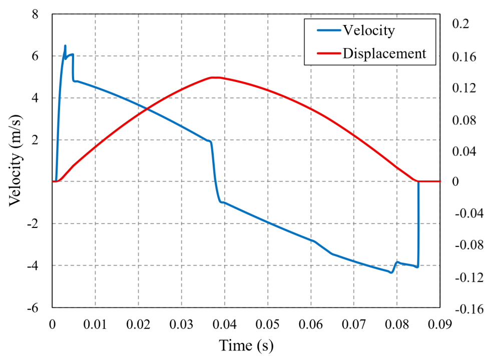

Fig. 9 Displacement and velocity of the breech

The calculated peak pressure inside the barrel is 285.28 MPa (see Fig. 8), while the reference value given in [20] is 281 MPa, resulting in a relative error of 1.5 %. The calculated firing cycle is 0.0849 seconds (see Fig. 9), corresponding to a theoretical rate of fire of 706 shots/minute. In paper [19], an experimental study was conducted to determine the motion profile of the bolt carrier in the AKM submachine gun. According to the experimental results [19], the firing cycle was 0.0846 s, corresponding to a theoretical rate of fire of 709 shots/min, with a relative error of 0.42 %. This comparison confirms that the theoretical simulation is reliable and can be effectively used in subsequent stability analyses.

One of the principal parameters used to evaluate the stability, operational safety, and reliability of the robot–weapon system is the robot displacement (Figs 10 and 11), the muzzle rise angle in the vertical plane (Fig. 12), and the muzzle swing angle in the horizontal plane (Fig. 13). These results were obtained through simulation under the single-shot firing mode.

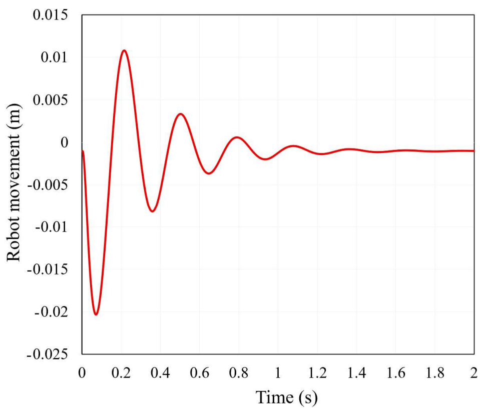

Fig. 10 Longitudinal displacement X-axis

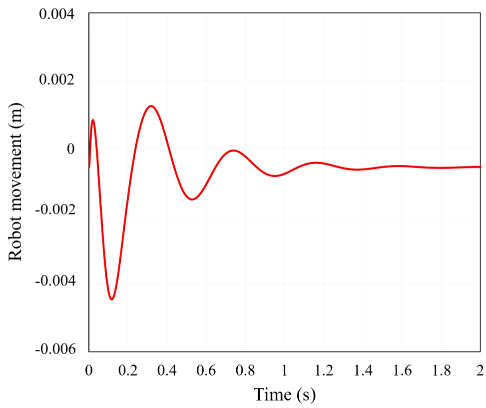

Fig. 11 Longitudinal displacement Z-axis

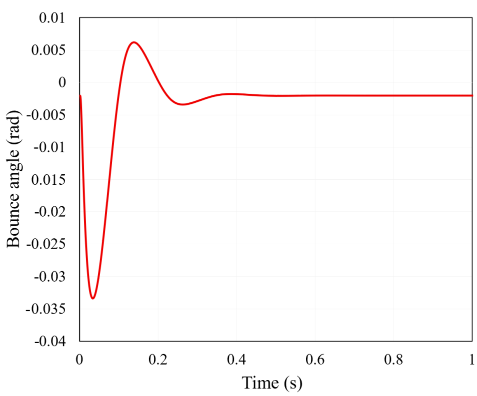

Fig. 12 Bounce angle Y-axis

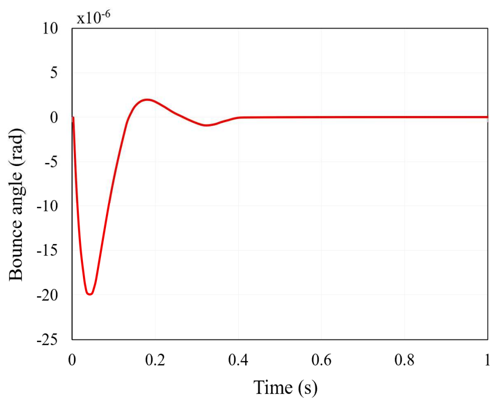

Fig. 13 Bounce angle X-axis

4 Influence of Certain Structural Parameters on Firing Stability

From the graphs in Fig. 10 to Fig. 13, it is observed that the longitudinal displacement of the robot along the X-axis has a maximum amplitude of 0.021 m, which is greater than the longitudinal displacement along the Z-axis, with a maximum amplitude of 0.0043 m. The angular displacement of the robot about the Y-axis reaches a maximum amplitude of 34×10^{-3} rad, whereas the angular displacement about the X-axis has a maximum amplitude of 20×10^{-6} rad, significantly smaller than that around the Y-axis. Therefore, when investigating the effects of structural parameters on firing stability, the focus is on the primary components that cause vibrations in the mechanical system. A study was conducted to evaluate the influence of selected structural parameters on the vibration response of the robot–weapon system during a three-round short burst firing mode.

4.1 Influence of Robot Mass

The mass of the robot body is 40 kg. The study was conducted by increasing the mass of the robot body by 5 kg, 10 kg and 15 kg. The results of this investigation are presented in Figs 14 and 15.

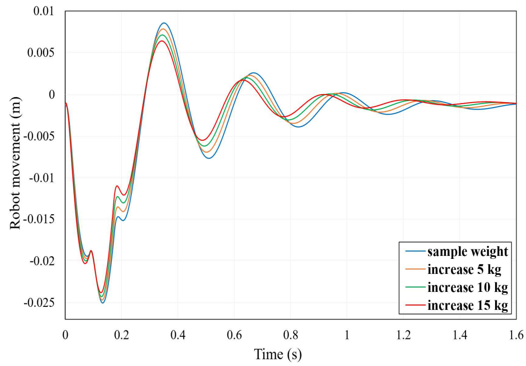

Fig. 14 Influence of mass on the robot's longitudinal displacement along the X-axis

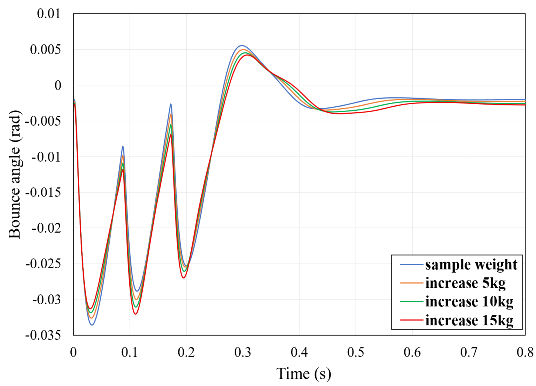

Fig. 15 Influence of mass on the robot's angular displacement about the Y-axis

The mass of the robot body has a significant effect on both the longitudinal and angular displacements of the robot in the vertical plane. When the robot body mass is increased by 5 kg to 15 kg, the maximum amplitude of the robot's longitudinal vibration decreases by 8.3 %, while the maximum amplitude of vibration in the opposite direction decreases by 33.7 % (Fig. 14). The maximum amplitude of the robot's muzzle rise angular vibration in the vertical plane decreases by 9.7 %, and the maximum amplitude of the opposite angular vibration decreases by 7.5 % (Fig. 15). Therefore, increasing the mass of the robot body enhances system stability and anti-rollover capability, resulting in reduced vibrations during firing. However, increasing the robot body mass also reduces the maneuverability and agility of the weapon system, posing difficulties when the robot navigates in complex or confined terrains.

4.2 Influence of Bore Axis Height

The bore axis height is defined as the vertical distance from the ground (or a designated reference plane) to the barrel axis (centerline of the barrel) when the robot is in the firing-ready position. To investigate the effect of bore axis height (dimension *h* in Fig. 2) on the vibration behavior of the robot–weapon system, the height (*h*) was incrementally increased to 0.82 m, 0.87 m, 0.92 m, and 0.97 m. The results of this investigation are presented in Figs 16 and 17.

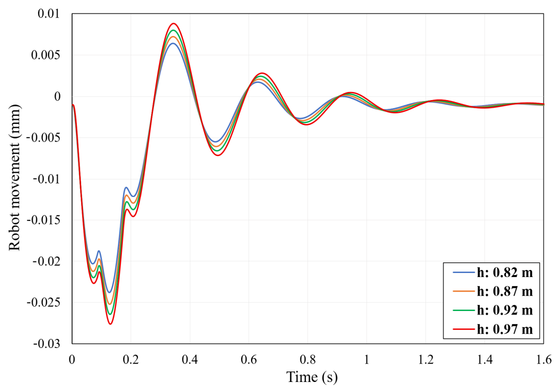

Fig. 16 Influence of bore axis height on the robot's longitudinal displacement along the X-axis

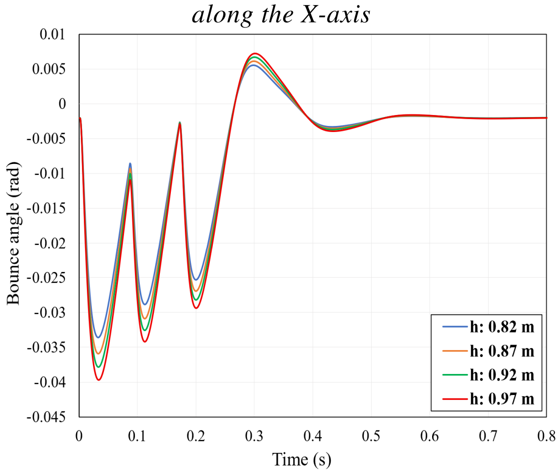

Fig. 17 Influence of bore axis height on the robot's angular displacement about the Y-axis

The bore axis height (h) has a relatively significant influence on both the longitudinal and angular displacements of the robot in the firing plane. When the bore axis height is increased from 0.82 m to 0.97 m, the vibration of the robot-weapon system also increases. Specifically, the maximum amplitude of the robot's longitudinal vibration increases by 11.1 %, and the amplitude of the backward vibration increases by 33.2 % (Fig. 16). The maximum amplitude of the robot's muzzle rise angular vibration in the vertical plane increases by 15.4 %, while the amplitude of the reverse angular vibration increases by 20.5 % (Fig. 17). Therefore, increasing the bore axis height is unfavorable for the firing stability of the robot. However, a higher bore axis can improve visibility and firing angles when the robot operates in complex terrain conditions.

4.3 Influence of Weapon Mount Center of Mass Position

The optimal mounting position of the weapon must be selected to ensure balance, stability, and combat effectiveness of the robot-weapon system. The weapon's center of mass should be positioned to prevent the robot from tipping over while maintaining mobility and rotational flexibility. In addition, the weapon mount should minimize recoil-induced vibrations, ensure system stability under firing forces, and optimize the firing angle, field of coverage, and control capabilities. To evaluate the effect of the weapon mounting position on the vibration behavior of the entire system, a study was conducted by varying the parameter (a from 0.1 m to 0.25 m (Fig. 3)). The weapon is mounted at the robot's center of mass, that is, when a equals b (Fig. 3). The results of this investigation are presented in Figs 18 and 19.

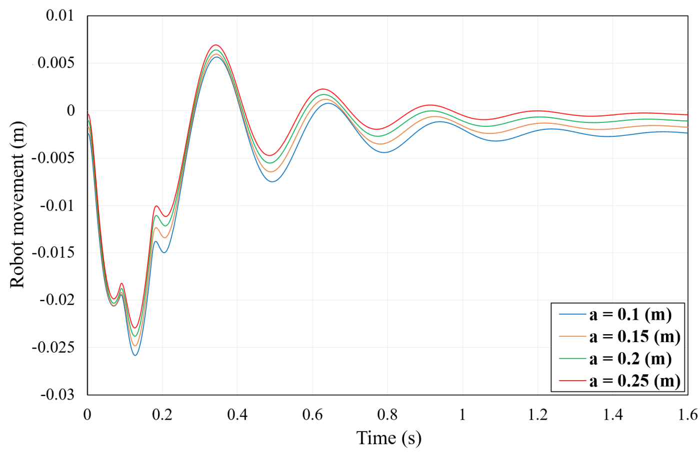

Fig. 18 Influence of weapon mounting position on the robot's longitudinal displacement along the X-axis

The weapon mounting position has a significant impact on both the longitudinal and angular displacements of the robot in the firing plane. When the parameter (a) is increased from 0.1 m to 0.25 m, the maximum amplitude of the robot's longitudinal displacement decreases by 11.5 % (Fig. 18). The maximum amplitude of the robot's muzzle rise angular vibration in the firing plane decreases by 4.7 %, and the amplitude of the reverse angular vibration decreases by 24.6 % (Fig. 19). These results indicate that positioning the weapon closer to the robot's center of mass contributes to improved system stability during firing.

The selection of appropriate structural parameters for the combat robot must not only satisfy the initial tactical and technical requirements, but also ensure the overall stability of the system under firing-induced forces.

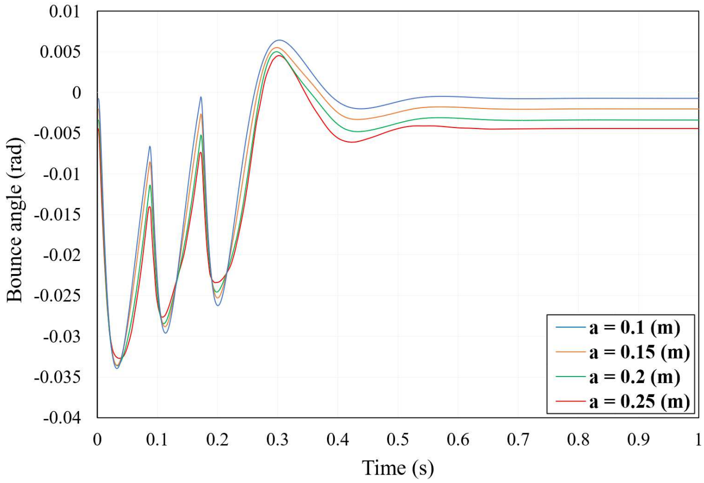

Fig. 19 Influence of weapon mounting position on the robot's angular displacement about the Y-Axis

5 Discussion

The obtained results clearly indicate that the firing stability of the robot-weapon system is strongly influenced by key structural parameters, namely the robot mass, the height of the bore axis, and the relative position of the weapon with respect to the robot's center of gravity. These parameters directly affect the dynamic response of the system during firing. The robot system tends to exhibit improved firing stability when the robot mass is increased, the height of the bore axis is reduced, and the weapon is mounted closer to the robot's center of gravity.

Specifically, increasing the robot mass by 37.5 %, which effectively raises the overall inertia of the coupled robot-weapon system, leads to a 33.7% reduction in the maximum vibration amplitude. In contrast, increasing the height of the line of fire by 18.3 % enlarges the moment arm of the recoil force relative to the ground contact points, resulting in higher pitching moments and intensified system vibrations; consequently, the maximum vibration amplitude increases by 33.2 %. Furthermore, when the weapon is mounted farther away from the robot's center of gravity, the recoil force generates larger overturning moments, thereby amplifying angular oscillations. The results indicate that shifting the weapon mounting position an additional 0.15 m away from the robot's center of gravity causes a 24.6 % increase in the maximum angular recoil amplitude of the system.

The presented results emphasize the importance of selecting optimal structural parameters for the robot-weapon system when firing on an elastic ground. By appropriately increasing the robot mass, lowering height of the bore axis, and positioning the weapon closer to the robot's center of mass, the adverse vibrations induced by firing forces can be effectively reduced, thereby improving firing stability.

6 Conclusions

The firing stability of automatic weapons mounted on ground combat robots has a significant impact on shooting accuracy. During firing, increased system stability leads to improved firing accuracy. The dynamic simulation of the UGV robot mechanical system, accounting for its actual spatial vibrations, represents the most general problem in the study of automatic weapon dynamics integrated into combat robots. This paper presents a method for determining several indicators to evaluate the firing stability of automatic weapons mounted on robots through modeling based on the multibody dynamics theory. A spatial dynamic model is developed for a small-caliber automatic weapon, consisting of five rigid bodies with six degrees of freedom, firing in short bursts. By applying the dynamic model and formulating the system's equations of motion during firing as described above, we are able to more accurately analyze and evaluate the effects of firing on the system's stability in both single-shot and burst-fire modes. The results of the study serve as a crucial foundation for further research into the influence of structural parameters on the firing stability of robot-mounted weapon systems, and provide an effective tool for new system design or structural optimization of existing robotic platforms, as well as for the system UGVs in the future.

Further experimental studies will evaluate the reliability of the theoretical dynamic model as a foundational basis for research aimed at improving the firing stability and accuracy of the robot-weapon system during operation.

References

[1] BALLA, J. Dynamics of Mounted Automatic Cannon on Track Vehicle. *International Journal of Mathematical Models and Methods in Applied Sciences*, 2011, **5**(3), pp. 423-432. ISSN 1998-0140.

[2] BALLA, J. Combat Vehicle Vibrations During Fire in Burst. In*: The Proceedings of International Conference on Mathematical Models for Engineering Science (MMES'10)*. Puerto De La Cruz: WSEAS Press, 2010, pp. 207-212. ISBN 978-960-474-252-3.

[3] SUN, H.K., Y.T. LIU and C.G. CHEN. Dynamic Analysis of a Vehicular-Mounted Automatic Weapon – Planar Case. *Defence Science Journal*, 2009, **59**(3), pp. 265-272. DOI 10.14429/dsj.59.1520.

[4] BALLA, J. and Z. KRIST. Infantry Fighting Vehicle in Case of Burst Firing. In: *2015 International Conference on Military Technologies*. Brno: IEEE, 2015. DOI 10.1109/MILTECHS.2015.7153661.

[5] SHI, Y.D. and D.S. WANG. Multi-Body Modeling and Vibration Analysis for Gun. In: *2009 International Conference on Intelligent Computing and Intelligent Systems*. Shanghai: IEEE, 2009, pp. 636-640. DOI 10.1109/ICICISYS.2009.5358333.

[6] APAROW, V.R., K. HUDHA, M.M. HAMDAN and S. ABDULLAH. Study on the Dynamic Performance of Armored Vehicle in Lateral Direction Due to Firing Impact. *Advances in Military Technology*, 2015, **10**(2), pp. 5-20. ISSN 2533-4123.

[7] VU, C.H. *Mechanics of Multibody Systems* (in Vietnamese). Hanoi: People's Army Publishing House, 2013.

[8] BALLA, J., M.H. DAO, T.H. TRUONG, V.D. NGUYEN and V.T. TRAN. Firing Stability of Automatic Grenade Launcher Mounted on Tripod. In: *2021 International Conference on Military Technologies*. Brno: IEEE, 2021. DOI 10.1109/ICMT52455.2021.9502836.

[9] TRUONG, T.H., M. MACKO, D.P. NGUYEN and D.T. VU. Effect of Some Structural Parameters on the Firing Stability of the PKMS Machine Gun when Firing with Complicated Boundary Conditions. In: *2021 International Conference on Military Technologies*. Brno: IEEE, 2021. DOI 10.1109/ICMT52455.2021.9502820.

[10] SHABANA, A.A. *Dynamics of Multibody Systems*. 5th ed. Cambridge: Cambridge University Press, 2020. ISBN 978-1-10-848564-7.

[11] VO, V.B., S. BEER, N.T. SY and N.D. PHON. The Effect of the Nozzle Ultimate Section Diameter on Interior Ballistics of Hv-76 Trial Gun. In: *2019 International Conference on Military Technologies*. Brno: IEEE, 2019, pp. 1-6. DOI 10.1109/MILTECHS.2019.8870040.

[12] WONG, J.Y. *Theory of Ground Vehicles*. 5th ed. Hoboken: Wiley, 2022. ISBN 978-1-119-71970-0.

[13] TRUONG, T.H. *Investigation of the Influence of Several Basic Parameters on the Stability of a Heavy Machine Gun During Firing* (in Vietnamese) [PhD Thesis]. Hanoi: Military Technical Academy, 2008.

[14] NGUYEN, D.P. and M. MACKO. Research Technical Solution for Reducing Oscillations of Weapons Mounted on the Vehicle. In: *2021 International Conference on Military Technologies*. Brno: IEEE, 2021. DOI 10.1109/ICMT52455.2021.9502835.

[15] BALLA, J., Z. KRIST, P.M. NGUYEN and B.V. VO. Study Effects of Shock Absorbers Parameters to Recoil of Automatic Weapons. In: *International Conference on Military Technologies 2021*. Brno: IEEE, 2021. DOI 10.1109/ICMT52455.2021.9502825.

[16] VO, B.V., T.V. PHUC and M. MACKO. Effect of Some Structural Parameters on Firing Stability of Shooter-Weapon System. *Advances in Military Technology*, 2021, **16**(2), pp. 235-251. DOI 10.3849/aimt.01487.

[17] BALLA, J. Contribution to Determining of Load Generated by Shooting from Automatic Weapons. In: *International Conference on Military Technologies.* Brno: IEEE, 2019. DOI 10.1109/MILTECHS.2019.8870116.

[18] TIEN, V.D., M. MACKO, S. PROCHÁZKA and V.V. BIEN. Mathematical Model of a Gas-Operated Machine Gun. *Advances in Military Technology*, 2022, **17**(1), pp. 63-77. DOI 10.3849/aimt.01449.

[19] NGUYEN, P.M., B.V. VO, D.V. DAO and D.V. NGUYEN. Studying the Dynamic Characteristics of Gas-Operated Guns Using SolidWorks Motion Software. *Vojnotehnički Glasnik/Military Technical Courier*, 2024, **72**(3), pp. 1066-1092. DOI 10.5937/vojtehg72-50987.

[20] TRAN, D.D. *Internal Ballistics Exercises* (in Vietnamese). Hanoi: Military Technical Academy, 2006.